

Effect of Interfacial Reaction on the Tensile Strength of Sn-3.5Ag/Ni-P and Sn-37Pb/Ni-P Solder Joints

Z. CHEN,^{1,3} M. HE,¹ A. KUMAR,¹ and G.J. QI²

1.—School of Materials Science & Engineering, Nanyang Technological University, Singapore, 639798, Singapore. 2.—Singapore Institute of Manufacturing Technology, Singapore, 638075, Singapore. 3.—e-mail: aszchen@ntu.edu.sg

This work investigates the effect of interfacial reaction on the mechanical strength of two types of solder joints, Sn-3.5Ag/Ni-P and Sn-37Pb/Ni-P. The tensile strength and fracture behavior of the joints under different thermal aging conditions have been studied. It is observed that the tensile strength decreases with increasing aging temperature and duration. Associated with the tensile strength decrease is the transition of failure modes from within the bulk solder in the as-soldered condition toward failures at the interface between the solder and the intermetallic compounds (IMCs). For the same aging treatment, the strength of the Sn-3.5Ag/Ni-P joint degrades faster than that of Sn-37Pb/Ni-P. The difference between the two types of joints can be explained by the difference in their interfacial reaction and growth kinetics. An empirical relation is established between the solder joint strength and the Ni₃Sn₄ intermetallic compound thickness.

Key words: Lead-free solder, electroless nickel, intermetallic compound (IMC), tensile strength

INTRODUCTION

In conventional flip chip packages, the electrical connection and mechanical integration between the integrated circuit (IC) chip and the substrate are realized with solder bumps. These solder bumps are connected to the I/O pads of the IC chip through under bump metallization (UBM) on one side and, on the other side, to the matching pads of the circuits on the substrate. The failure of a single solder joint can render malfunction to a device, or even an entire electrical system. Therefore, reliability of solder joints in flip chip packages has become a critical aspect of electronic circuit reliability.

The UBM is a layer or layers of thin film metals deposited on the IC pads to protect the IC metallization from being attacked by the solder and, at the same time, to provide a good wetting surface to the solder. High lead content Sn-Pb solder bumps were successfully used with Cr-Cu UBM in C4 (control collapse chip connection) technology by IBM in the 1960s.¹ Because of the concerns of environmental

pollution by lead, lead-free solders have replaced Pb-containing solders^{2,3} in recent years. However, all of the usable lead-free solders contain a high amount of tin and, similar to the eutectic Sn-Pb alloy, were found to be incompatible with Cu-based UBMs due to the rapid consumption of copper film in the UBMs and spalling of Cu-Sn intermetallic compounds (IMCs).⁴⁻⁷ As alternatives, Ni-based UBMs, such as electrolessly plated Ni-P alloy (EN) and sputtered pure Ni, have been reported to have slower reactions with the high-Sn solders^{6,8} with fairly good wettability.⁹ Among them, electroless Ni-P, which is actually an amorphous alloy of Ni with 6–13wt.%P, has attracted a great deal of attention because of its low process cost and other merits.^{6,10,11} However, the inevitable introduction of P during plating complicates the solder reaction at the interface, which makes the reliability assessment more complicated.

Many studies have been devoted to the interface IMC morphology and growth kinetics between Ni-P and Sn-bearing solders.^{10,12-26} Studies on the joint strength were mainly carried out by shear test.²⁴⁻²⁶ Relatively less work has been done on the strength

of the joint by tensile test. The shear test has been routinely performed by the packaging industry, because it closely reproduces the stress state in a real package. However, we chose to use the tensile test in the current study, primarily for the purpose of preserving the fractured surface for fractographic analysis. Another distinct feature of the tensile test is that the stress distribution in all interface layers is the same, so the test can be used to reveal the weakest layer or interface.²⁷

In the present work, tensile testing and the fracture behavior of Sn-3.5Ag/Ni-P and Sn-37Pb/Ni-P joints in different thermal aging conditions were investigated, and the influence of interface reaction and solder composition on the solder joint strength will be discussed.

EXPERIMENTAL PROCEDURES

Ni (99%) plates of 2.0-mm thickness were used as substrate for the plating of electroless nickel. The plates were polished to an optical finish on the to-be-joined surfaces, and then solvent degreased and cleaned in deionized water before subsequent electroless nickel plating. A Ni-P (7wt.%P) layer of about 5- μm thickness was obtained with a commercial solution. A final finish of immersion gold on the plated Ni-P was applied for surface protection.

Figure 1 shows the schematic drawing of the fixture that holds together the plated Ni plates to be soldered. First, the surfaces of Ni-P coatings on each of the Ni plates were coated with rosin mildly activated flux. An excessive amount of the Sn-3.5Ag (or Sn-37Pb) solder was then put in between the two carefully aligned plates. The distance between the parallel surfaces facing each other was maintained at 0.8 mm. The specimen setup was sent into a reflow oven, heated to 251°C, and held at that temperature for 180 s for the Sn-3.5Ag solder or at 213°C for 120 s for the Sn-37Pb solder. The specimen setup was finally taken out of the oven and cooled in air. The cooling temperature profiles were

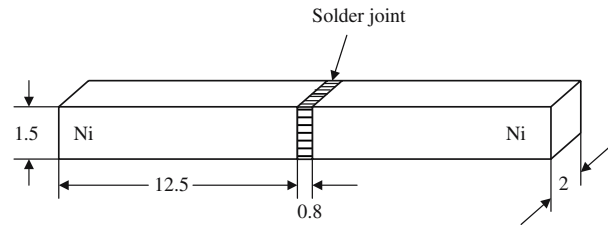


Fig. 2. Dimensions of the tensile testing specimen used in the current work. The dimensions are in millimeters.

obtained through a thermocouple attached to the sample. The average postreflow cooling rate was calculated from the temperature profiles from the melting point to 30°C below the melting point. The cooling rate was found to be between 3.0°C/s and 5.0°C/s for both types of joint. After joining, excessive solder flowing out of the solder joint area was carefully ground away. The as-soldered specimens were cut, using a diamond precision cutter, into small pieces with rectangular cross sections with dimensions of 1.5 mm \times 2.0 mm. The dimensions of the final tensile testing specimen used in this study are shown in Fig. 2.

The as-soldered tensile test specimens were thermally aged at 150°C and 170°C for 100 h, 225 h, 400 h, and 625 h. Three samples from each condition were tested using an Instron 5567 tester at room temperature with a constant crosshead speed of 0.5 mm/min. Force and displacement were recorded. A JEOL JSM-6360A (Japan Electron Optics Ltd., Tokyo) scanning electron microscope (SEM) was used to observe both the cross-sectional microstructure of the joint and the top view of the fractured surface. The elemental composition of the fracture surfaces was characterized in the SEM using energy-dispersive x-ray (EDX) analysis. After the tensile test, all samples were observed on the broken surfaces under the SEM. The microstructure and fracture path were observed by cross-sectioned SEM, from which the IMC thickness was obtained for each condition. In order to quantify the IMC thickness with good precision, image analysis software was used to measure the area and length of IMCs in cross-sectional SEM images. The average thickness of the IMC layer was calculated using the measured area divided by the length in the area.

RESULTS

Microstructure at the Joint Interface

The cross-sectional view of the interfacial microstructure for the Sn-3.5Ag joint is shown in Fig. 3. In the as-reflow state, the Ni_3Sn_4 IMC consisted of needlelike and chunky grains (Fig. 3a) with an average thickness around 2 μm . After aging, the IMC layer became thicker and relatively smooth (Fig. 3b). In comparison, the interface IMC in the Sn-37Pb/Ni-P joint had more needlelike spikes in the as-reflow state (Fig. 4a), and the average

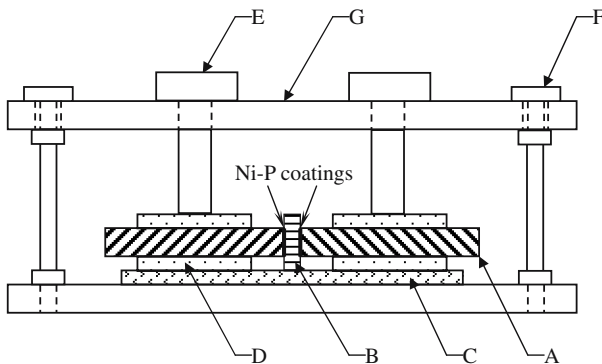


Fig. 1. Schematic diagram for solder joint making. Description of labels in the figure: A—Ni plate with Ni-P coating, B—solder, C—ceramic pad, D—spacer, E and F—screws, and G—clamping plate.

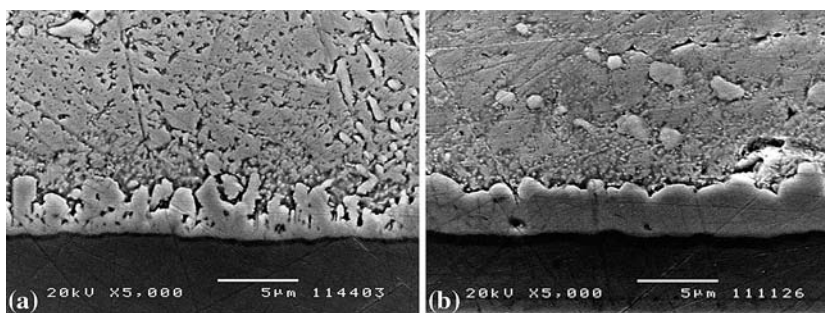


Fig. 3. Cross-sectional view of the Sn-3.5Ag/Ni-P joint: (a) reflowed at 251°C for 180 s and (b) thermally aged at 150°C for 625 h.

thickness was thinner than that of the Sn-3.5Ag joint. After aging, the IMC in the Sn-37Pb/Ni-P joint also became smooth and thickened in a similar way (Fig. 4b). Microstructure coarsening of the bulk solder could be easily observed in the case of Sn-37Pb/Ni-P joint, as shown in Fig. 4b, due to the contrast between Pb-rich phase (in light color) and the rest of the bulk solder. This also shows that the Pb-rich phase segregated at the interface during aging.

Tensile Strength of Solder Joints

The tensile strengths of the solder joints aged in different thermal aging processes are listed in Table I and plotted in Fig. 5. The average ultimate tensile strength (UTS) of the as-soldered Sn-3.5Ag/Ni-P joint was 76.3 MPa. The UTS for as-soldered Sn-37Pb/Ni-P joint was 76.1 MPa. It can be seen from Fig. 5 that the strength of the Sn-3.5Ag/Ni-P joint dropped continuously with the increase of aging time, and the drop was greater when the aging temperature was higher. The degradation of tensile strength for the Sn-37Pb/Ni-P solder joints was greater during the first 100–200 h. Further extension of the aging time resulted in a quite minimum decrease in UTS. For example, after aging at 170°C for 100 h, the tensile strength dropped to 63.2 MPa from 76.1 MPa of the as-reflowed state. When the aging duration extended to 625 h, the tensile strength of the Sn-37Pb/Ni-P solder joint was still 58.9 MPa. The thermal aging temperature also showed less effect on the tensile

strength of Sn-37Pb/Ni-P solder joints. There was no obvious difference in tensile strength between the specimens aged at 150°C and 170°C when the aging duration exceeded 225 h.

Fractographic Analysis

Sn-3.5Ag/Ni-P joint

Figure 6a is the SEM micrograph showing the cross-sectional view of the complete failure path of the as-soldered Sn-3.5Ag/Ni-P solder joint. There was clear necking in the bulk solder, and the reduction in the specimen width was about 5%. The fracture surface was inclined at about 45° to the tensile-stress axis. The fractured surface in Fig. 6b showed quasi-cleavage facets with many shear lips, indicating a mixture of microscopic brittle and ductile fractures. The entire crack was inside the bulk solder. This means that the joint strength for as-reflowed test specimens was controlled by the cohesive strength of the Sn-3.5Ag solder. The interfacial intermetallic compound layer itself and its adhesion to both solder and substrate were stronger than the strength of the bulk solder.

When aged at 150°C for 100 h, the fracture behavior of the Sn-3.5Ag/Ni-P solder joint was similar to those of the as-soldered specimens. With further extension of aging at the same temperature, the fracture path turned into a mixed bulk solder and interface failure, and the percentage of failure inside the bulk solder decreased with aging time. When aged for 625 h at 150°C, the fracture occurred

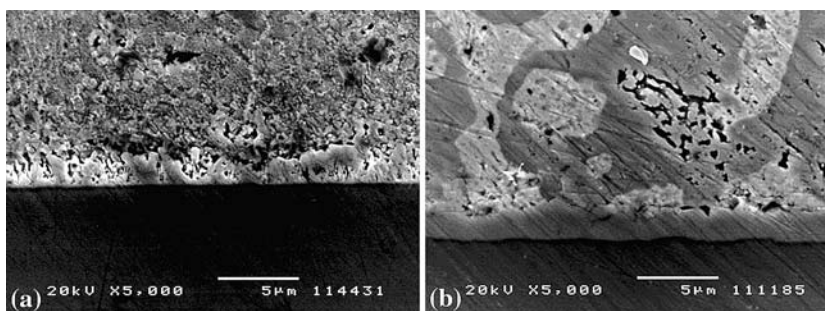


Fig. 4. Cross-sectional view of the Sn-37Pb/Ni-P joint: (a) reflowed at 213°C for 120 s and (b) thermally aged at 150°C for 625 h.

Table I. UTS and Ni_3Sn_4 Thickness for the Two Types of Solder Joints.

Aging Time, h		Sn-3.5Ag/Ni-P		Sn-37Pb/Ni-P	
		150°C	170°C	150°C	170°C
0	Strength (MPa)	76.3		76.1	
	Thickness (μm)	2.10		1.30	
100	Strength (MPa)	74.8	67.9	74.2	63.2
	Thickness (μm)	2.61	2.99	1.61	1.97
225	Strength (MPa)	72.1	51.6	64.8	64.7
	Thickness (μm)	2.89	3.53	1.83	2.39
400	Strength (MPa)	64.7	45.8	61.3	61.4
	Thickness (μm)	3.04	4.01	1.91	2.70
625	Strength (MPa)	51.5	44.3	61.1	58.9
	Thickness (μm)	3.66	4.33	2.10	3.16

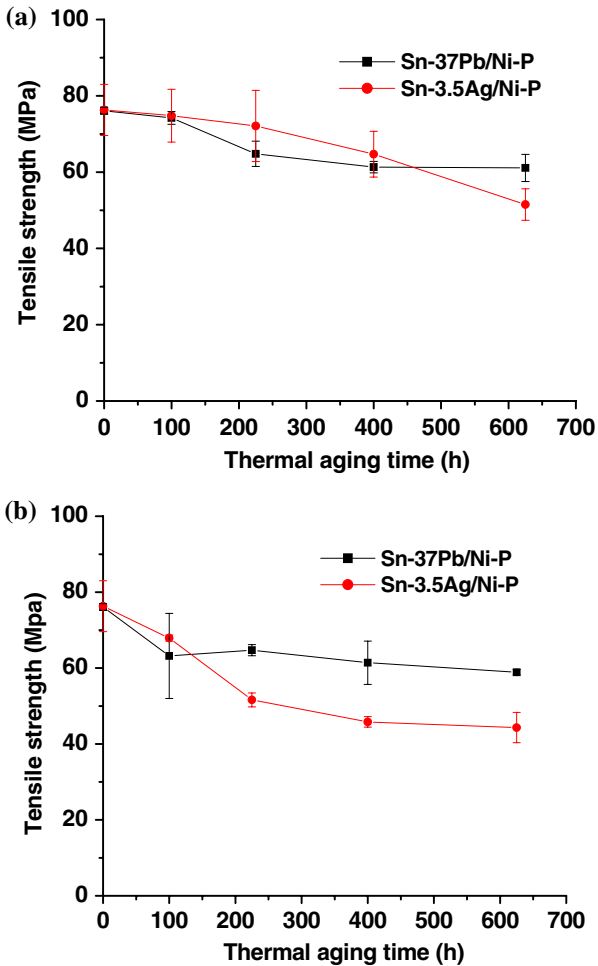


Fig. 5. Tensile strength for the thermally aged solder joints at different temperatures: (a) 150°C and (b) 170°C.

completely at the IMC/solder interface, as shown in Fig. 7. Figure 8 reveals that the separation at the interface was between the IMCs and the bulk solder. Shallow dimples formed as a result of IMCs delaminated from the solder. The EDX analysis on

the broken surfaces further confirmed that the failure was indeed between the Ni_3Sn_4 IMCs and the solder. The fracture behavior of Sn-3.5Ag/Ni-P solder joints at 150°C can be summarized as follows: the fracture was inside the bulk solder and macroscopically ductile for 100 h aged samples. It was completely interfacial and macroscopically brittle after a 625 h aging treatment. In between the two, the fracture was mixed bulk solder failure and interface failure.

When Sn-3.5Ag/Ni-P solder joints were thermally aged for 100 h at 170°C, failure was predominantly at the solder/ Ni_3Sn_4 interface with a small percentage in the bulk solder. The whole fracture surface was relatively flat, indicating macroscopically brittle behavior. When the aging duration was 400 h at 170°C, the crack still propagated, mainly along the interface between the Ni_3Sn_4 and solder, but at some locations, it turned inside the Ni_3Sn_4 layer, causing brittle, intergranular fracture of the intermetallics. Figure 9 shows the transition from the solder/ Ni_3Sn_4 interface to the IMC layer. For samples aged longer, for 625 h at 170°C, the crack path was similar to the 400 h sample, but the interfacial dimples were larger and shallower, indicating increased brittleness at microscopic scale.

Sn-37Pb/Ni-P joint

The failure path of as-soldered Sn-37Pb/Ni-P joints was also inside the bulk solder, as shown in Fig. 10. The necking (>10% reduction in width) was apparently greater than in the as-soldered Sn-3.5Ag/Ni-P joint, indicating a better ductility of Sn-37Pb solder. The SEM micrographs of the fracture surface in Fig. 10b also revealed deeper dimples on the fracture surface. This feature indicates that the Sn-37Pb solder is more ductile than the Sn-3.5Ag solder on a microscopic level.

For the thermally aged Sn-37Pb/Ni-P joints, tensile failure always occurred inside the bulk solder for specimens aged at 150°C for 100 h, 225 h, and

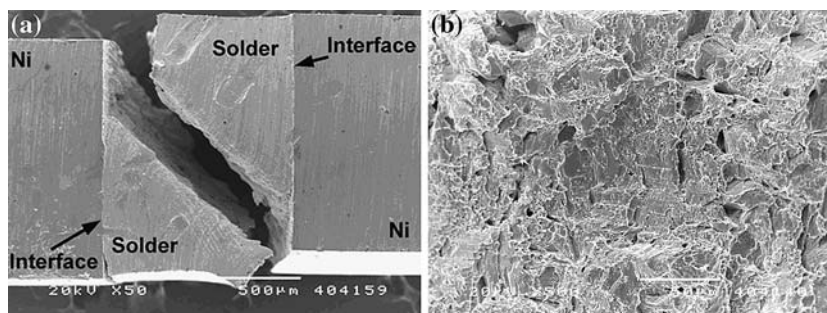


Fig. 6. Failure path and fracture surface of as-soldered Sn-3.5Ag/Ni-P specimens. (a) Cross-sectional view of the entire fracture joint. Note that necking has occurred in the bulk solder. (b) Quasi-cleavage fracture viewed from the fractured surface. The scale bar is 50 μm .

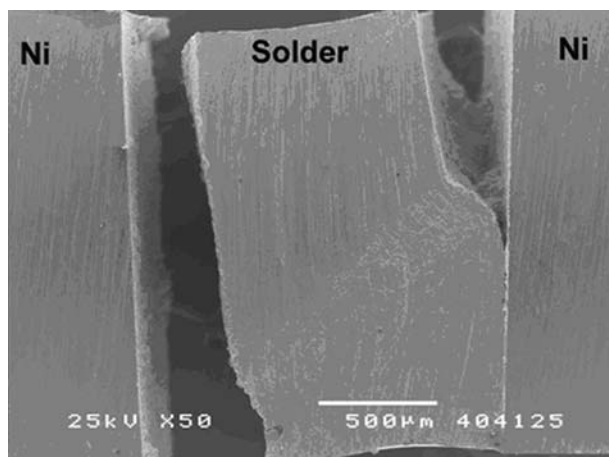


Fig. 7. Fracture path of Sn-3.5Ag/Ni-P solder joint aged at 150°C for 625 h.

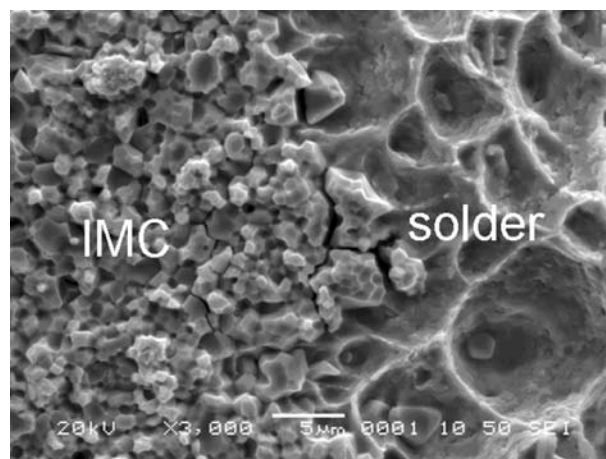


Fig. 9. Fracture surfaces in Sn-3.5Ag/Ni-P solder joints aged at 170°C for 400 h. The figure shows the transition of fracture from dimpled Ni_3Sn_4 /solder interface to intergranular cracking inside the Ni_3Sn_4 IMC layer.

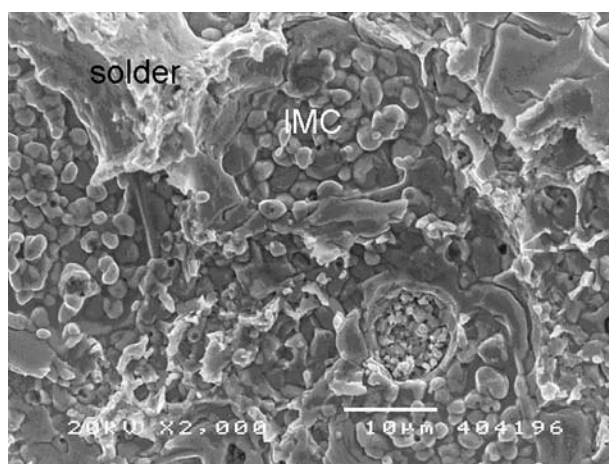


Fig. 8. Interface separation between the Ni_3Sn_4 compounds and the bulk solder. Large shallow dimples are observed on the fractured surface.

400 h, as well as at 170°C for 100 h. The failure paths were similar to those of as-soldered specimens. Bulk solders failed by about 45° to the joint plane, and necking occurred in the bulk solder, indicating a ductile failure process. The fracture surface showed dimpled morphology, as shown in

Figs. 11 and 12. The backscattering electron (BE) SEM micrographs of fracture surfaces (Figs. 11b and 12b) show the existence of Pb-rich phases in light color.

When the duration reached 625 h at 150°C or 225 h and 400 h at 170°C, the fracture path turned into the interface region, as shown in Fig. 13. No necking was observed in the bulk solder, indicating that the macroscopic behavior was largely brittle. There were many dimples on the fracture surface, as shown in Fig. 14. From EDX and SEM analyses on the broken surfaces on both sides, it was found that most of the fracture occurred inside the bulk solder. Ni_3Sn_4 was observed only at scattered locations. These dimples near the interface were deeper and smaller in size than those in the Sn-3.5Ag solder. This again shows that the Sn-37Pb solder has a higher ductility even when failure is macroscopically brittle. When this interfacial failure occurred, the volume of Pb-rich phases increased as a result of long-term aging treatment. Figure 14b is the BE SEM micrograph with the light colored area corresponding to the Pb-rich region.

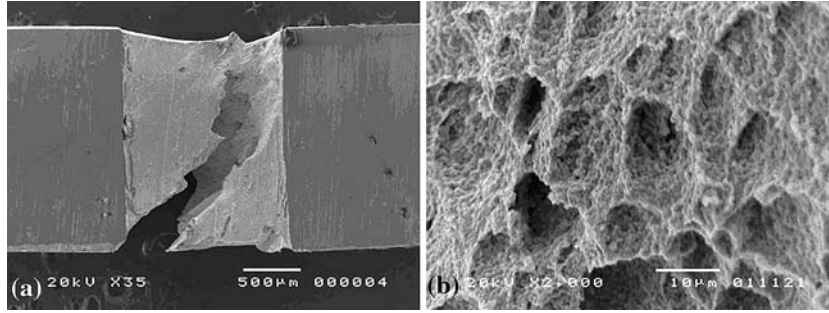


Fig. 10. Failure path of as-soldered Sn-37Pb/Ni-P solder joint. (a) Cross-sectional view of the entire fracture joint. Higher degree of necking in the bulk solder indicates that the solder is more ductile than Sn-3.5Ag. (b) Dimples observed from the fractured surface.

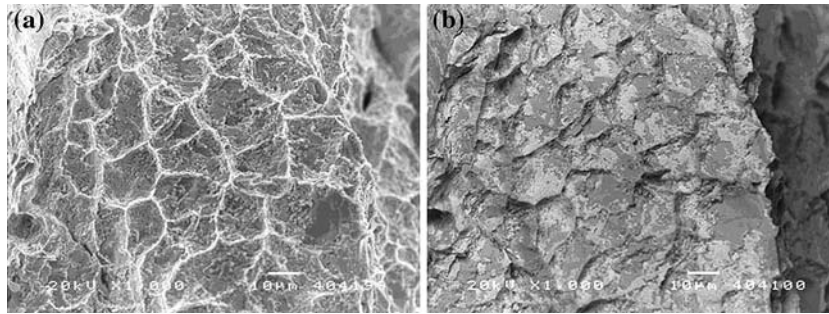


Fig. 11. Fracture surface in Sn-37Pb/Ni-P solder joints aged at 150°C for 100 h. (a) Secondary electron (SE) SEM micrograph and (b) BE SEM micrograph of (a).

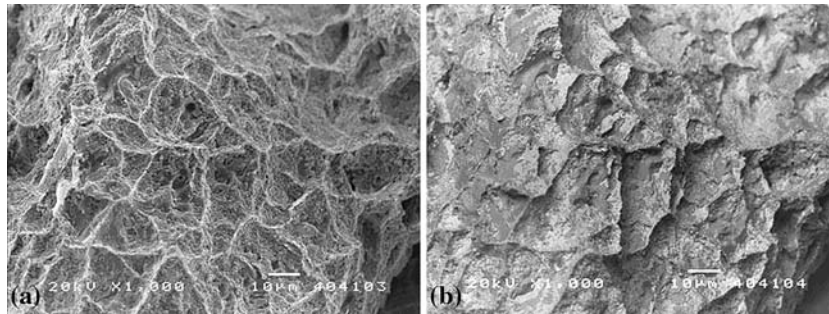


Fig. 12. Fracture surface in Sn-37Pb/Ni-P solder joints aged at 170°C for 100 h: (a) SE SEM micrograph and (b) BE SEM micrograph of (a).

An interesting difference between the Sn-3.5Ag and Sn-37Pb solder joints was observed. Although the macroscopic appearance of the interface failure was similar for both types of joints, microscopically, the crack path was mainly along the Ni_3Sn_4 IMC/solder borderline in the Sn-3.5Ag solder joint (Fig. 8). However, in the case of the Sn-37Pb solder joint, the crack path predominantly stayed within the Pb-rich layer near the interface. The observation shows that the Pb-rich phase, which segregates near the interface due to prolonged solder reaction, is comparatively weaker than the bulk solder away from the interface.

When aging duration increased to 625 h at 170°C, the crack path was a mixed solder/ Ni_3Sn_4 interface (Fig. 15) and inside the Ni_3Sn_4 layer (Fig. 16). The Pb-rich phase on the fracture surface increased

further as compared to specimens experiencing shorter aging duration. When failure was inside the Ni_3Sn_4 IMC layer, there were fine faceted Ni_3Sn_4 grains on the fracture surface of both the substrate and solder sides, as shown in Fig. 16.

DISCUSSION

Effect of Thermal Aging on Solder Joint Fracture Behavior

The fracture behavior of the solder joints is influenced by the interfacial reaction during the solid-state reaction. The tensile strength of the solder joint is dependent upon all structures in the joint, including the Ni_3Sn_4 intermetallic compound layer and other interfacial layers such as the Ni-Sn-P, Ni_3P , and Ni-P coating.^{21,22,23} From the obser-

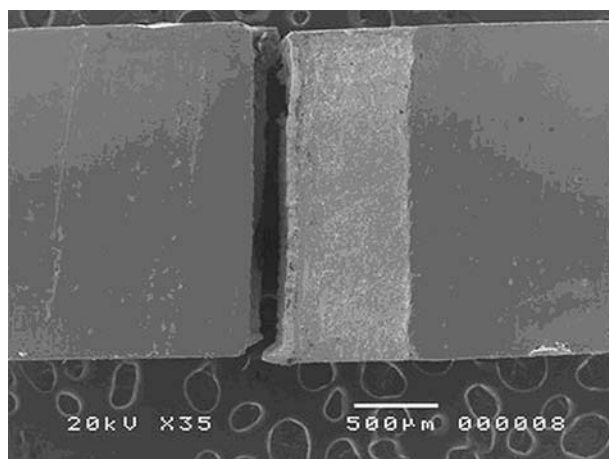


Fig. 13. Fracture path of Sn-37Pb/Ni-P solder joint aged at 170°C for 400 h.

vation made above, three typical fracture patterns could be summarized. These patterns are as follows: (1) ductile failure inside the bulk solder, (2) dimpled fracture at or near the solder/ Ni_3Sn_4 interface, and (3) failure inside the Ni_3Sn_4 layer. The general trend is that with extended aging time and increased aging temperature, the fracture mode moves from solder failure to interfacial failure with decreasing strength.

The weakening of the Ni_3Sn_4 /solder interface with aging time is a complex phenomenon and has always been a focus of interest.^{24–29} The phosphorus-rich layer was believed to be the cause of the weakening in shear strength found by Alam et al.^{24,25} In another study, the brittleness of Ni_3Sn_4 and formation of Kirkendall voids were also cited as reasons for the decrease of shear strength.²⁶ Relatively little research has been reported for tensile strength degradation. In the current work, a few possible reasons are discussed. One possible factor is the stresses that are generated between the interfacial layers and the solder during growth. The stresses could be originated by the volume mismatch between neighboring layers. Another factor may be the smoothening of the solder/IMC interface during thermal aging (comparing parts a and b of Figs. 3 and 4). At the as-reflow state, the solder/IMC interface is usually quite rough due to nonequilibrium phase formation and growth in short times (Figs. 3a and 4a). The IMC and solder penetrate each other. Therefore, even though stress concentration occurs at the interface, the actual crack path along the interlocked interface requires more energy and greater applied load compared to a flat interface. When the interface strength is higher than the ductile failure strength of the solder, failure occurs in the bulk solder. However, after long

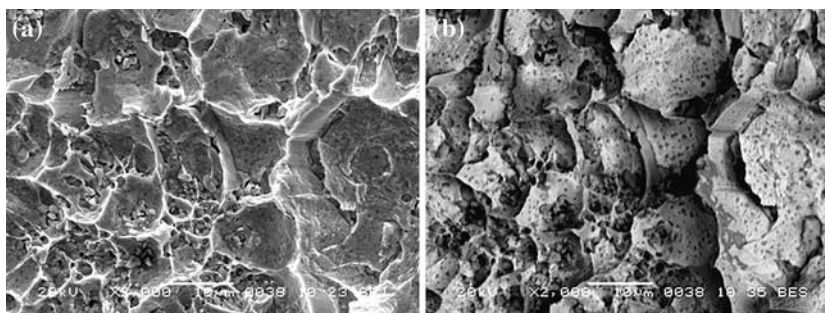


Fig. 14. Fracture surface in Sn-37Pb/Ni-P solder joints aged at 150°C for 625 h. The fracture occurs near the interface, but mainly stays in the solder. The IMCs are only visible at some spots. (a) SE SEM micrograph of fracture at solder/ Ni_3Sn_4 interface, substrate side; and (b) BE SEM micrograph of (a), showing Pb-rich phase in light color.

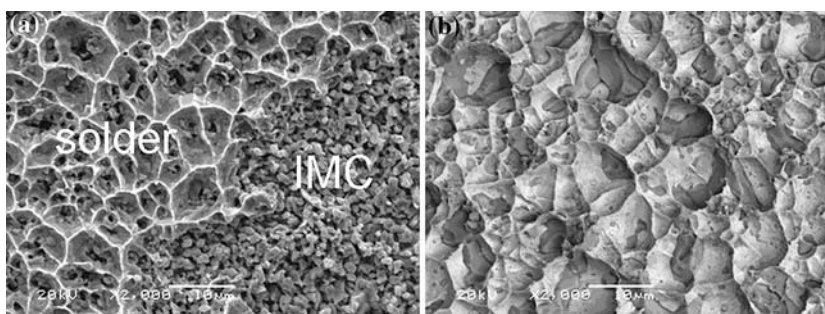


Fig. 15. Fracture surface in Sn-37Pb/Ni-P solder joints aged at 170°C for 625 h; failure between solder and Ni_3Sn_4 IMC layer. (a) Substrate side, SE; and (b) solder side, BE.

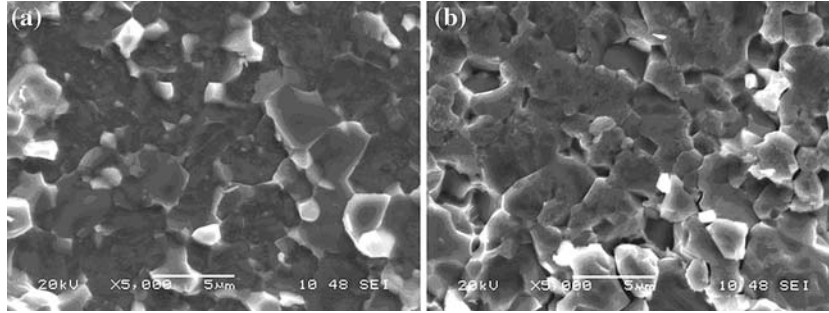


Fig. 16. Sn-37Pb/Ni-P solder joints aged at 170°C for 625 h: (a) viewed from the substrate side and (b) viewed from the solder side. The graphs show that the failure is inside the Ni_3Sn_4 IMC layer because cleaved IMCs are observed from both sides of the fracture.

time thermal aging, the interface becomes smoother due to the tendency of reducing the interface area. As a result, interface fracture strength is significantly reduced. Coupled with the mismatch stress built up, the interface failure mode becomes dominant with deeper aging.

With further interface reaction, the thickness of the Ni_3Sn_4 IMC increases. Fracture within the IMC layer becomes possible because of its brittle nature. The cracks that may initiate elsewhere (e.g., interface between the IMC/solder layers) could propagate into the IMC layer. This type of brittle fracture (in the IMC layer) has also been reported by other researchers^{28,29} From what we have observed, the sample usually shows combined IMC fracture and interface fracture modes. This is due to the complexity in microstructures and stress state at the interface.

From the above analysis, it is concluded that during thermal aging, the growth of interfacial layers greatly influences the tensile strength and fracture behavior of a solder joint. A good indication

of the extent of interfacial reaction is the Ni_3Sn_4 IMC thickness. The Ni_3Sn_4 thickness is incorporated with the tensile strength in Table I. Figure 17 shows a correlation between the IMC thickness and tensile strength of Sn-3.5Ag/Ni-P and Sn-37Pb/Ni-P solder joints under different thermal aging conditions. Data from the two types of solder joints are plotted together. When the fracture is inside the solder, the strength is always higher than 60 MPa, and the thickness of the Ni_3Sn_4 IMC is less than 3 μm . When the failure path moves to the interface, the tensile strength drops to 50–60 MPa and the Ni_3Sn_4 IMC thickness increases to 2.5–3.5 μm . When the brittle fracture of the Ni_3Sn_4 layer occurs, the fracture strength further drops to 40 MPa, and the corresponding Ni_3Sn_4 IMC thickness is around 4 μm . In both types of solder joints, there is a quite linear correlation between the joint strength and the IMC thickness (Fig. 17). Therefore, the thickness inspection could be used as an indication of joint strength.

Effect of Solder Composition on the Fracture Behavior of Solder Joints

During thermal aging, the tensile strength of the Sn-3.5Ag/Ni-P joints decreases faster than that of the Sn-37Pb/Ni-P solder joints, as can be seen from Fig. 5. Two factors related to solder composition might influence the strength and fracture behavior of different solder joints. The first factor is the reaction rate of solder with the Ni-P metallization, as manifested by the Ni_3Sn_4 IMC thickness. In Fig. 17, it is obvious that the relationship between IMC thickness and the tensile strength in the Sn-37Pb solder joint follows almost the same trend as that of the Sn-3.5Ag/Ni-P joint. The higher sensitivity of tensile strength to aging temperature and duration for the Sn-3.5Ag/Ni-P joint is due to the fast reaction rate of the Sn-3.5Ag solder with Ni-P. The second factor is the effect of the other element besides Sn in solders. For eutectic Sn-3.5Ag, the solidified bulk solder consists of Sn with dendritic globules and interdendritic regions with a eutectic dispersion of Ag_3Sn precipitates.³⁰ For the eutectic Sn-37Pb solder, the existence of 37wt.%Pb

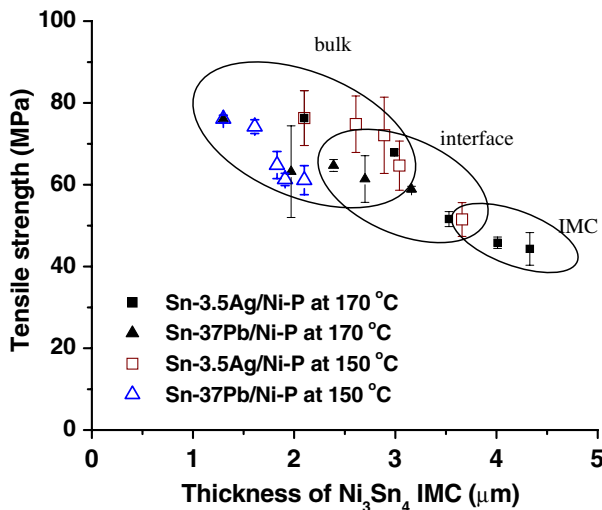


Fig. 17. Failure mechanisms and the relation between the tensile strength and Ni_3Sn_4 intermetallic thickness of thermally aged solder joints.

not only increases the ductile property of Sn⁷ but also influences the fracture behavior of the solder joint.^{31–33} The Pb-rich layer between the solder and the interfacial Cu₆Sn₅ IMC layer in Sn-37Pb/Cu solder joints was reported to be responsible for the interfacial separation between the solder and interfacial IMC layer.^{28,31,33} This is further confirmed by the present study. The Pb-rich phase was observed on both the substrate and solder sides of the broken surface on the fractured Sn-37Pb/Ni-P solder joint. The volume fraction of the Pb-rich phase increases with aging time. The accumulation of Pb at the interface of the solder and Ni₃Sn₄ is the result of continued reaction between Sn and Ni. The existence of the Pb-rich layer besides the brittle Ni₃Sn₄ IMC increases the discontinuity of mechanical properties at the interfacial area. Figure 14 provides evidence of ductile failure in the Pb-rich layer at the vicinity of the IMC/solder interface, which implies that the Pb-rich layer is weaker in strength.

CONCLUSIONS

The tensile strengths of thermally aged solder/Ni-P joints were measured with a specially designed fixture, and the fracture surface and failure behavior of these solder joints were analyzed. The effect of intermetallic compounds on the mechanical properties of these solder joints was also investigated. The following conclusions can be drawn.

1. The fracture behavior of the solder joint changes with thermal aging conditions. Failure may occur inside the bulk solder, the solder/IMC interface, and within the Ni₃Sn₄ IMC layer. With extended aging time and increase of aging temperature, the fracture mode shifts from the bulk solder failure to the interface and IMC fracture.
2. When the failure occurs in the bulk solder, both types of solder joints show macroscopic necking. The Sn-37Pb/Ni-P joint has a better ductility than Sn-3.5Ag/Ni-P. Either the interface separation at the IMC/solder interface of the Sn-3.5Ag/Ni-P joint or the Pb-rich layer failure of the Sn-37Pb/Ni-P joint is macroscopically brittle but microscopically ductile (dimples).
3. The degradation of tensile strength for thermally aged Sn-37Pb/Ni-P solder joints is slower than that of Sn-3.5Ag/Ni-P. The reason is that the interfacial reaction is much slower in the former. In extended aging, the Pb-rich phase accumulates close to the IMC/solder interface in the Sn-37Pb/Ni-P joint. The Pb-rich phase provides an easy fracture path within the bulk solder.
4. The thickness of intermetallic compounds provides a good indication of the tensile strength. The reason for such a good correlation is that the thickness variation closely relates to the interfacial reactions, on which weakening of the interface is dependent.

REFERENCES

1. J.H. Lau (1996) *Flip Chip Technologies* McGraw-Hill, New York.
2. N.A. Bruinsma, Lead-Free Soldering—Legislative Issues, the Road Towards Lead-Free Soldering (Eindhoven, Nov. 16, 2001).
3. WEEE, Directive of The European Parliament and of the Council on Waste Electrical and Electronic Equipment, on the Restriction of the Use of Certain Hazardous Substances in Electrical and Electronic Equipment (Brussels: Commission of The European Communities, 2000), pp. 59–83.
4. H.K. Kim, K.N. Tu, and P.A. Totta, *J. Appl. Phys. Lett.* 68, 2204 (1996).
5. A.A. Liu, H.K. Kim, and K.N. Tu, *J. Appl. Phys.* 80, 2774 (1996).
6. K.N. Tu and K. Zeng, *Mater. Sci. Eng.* R34, 1 (2001).
7. K. Zeng and K.N. Tu, *Mater. Sci. Eng.* R38, 55 (2002).
8. P.G. Kim, J.W. Jang, T.Y. Lee, and K.N. Tu, *J. Appl. Phys.* 86, 6746 (1999).
9. R.J.K. Wassink (1984) *Soldering in Electronics* Electrochemical Publications Ltd, Ayr, Scotland.
10. K.C. Hung, Y.C. Chan, and C.W. Tang, *J. Mater. Sci.: Mater. Electron* 11, 587 (2000).
11. P.L. Liu and J.K. Shang, *Metall. Mater. Trans.* A 31A, 2857 (2000).
12. A. Kumar, M. He, and Z. Chen, *Surface Coatings Technol.* 198, 283 (2005).
13. J.W. Jang, P.G. Kim, K.N. Tu, D.R. Frear, and P. Thompson, *J. Appl. Phys.* 85, 8456 (1999).
14. M. He, Z. Chen, G.J. Qi, C.C. Wong, and S. Mhaisalkar, *Thin Solid Films* 462, 363 (2004).
15. Y.D. Jeon and K.W. Paik, *IEEE Trans. Components Packaging Technol.* 25, 169 (2002).
16. C.Y. Lee and K.L. Lin, *Thin Solid Films* 249, 201 (1994).
17. M. He, W.H. Lau, G.J. Qi, and Z. Chen, *Thin Solid Films* 462, 376 (2004).
18. K.L. Lin and Y.C. Liu, *IEEE Trans. Adv. Packaging* 22, 568 (1999).
19. P.L. Liu and J.K. Shang, *J. Mater. Res.* 15, 2347 (2000).
20. Z. Mei and R.H. Dauskardt (1999) *MRS Spring Meeting Symposium M; Materials Reliability in Microelectronics IX* Materials Research Society, Pittsburgh, PA, pp 1–6.
21. M. He, Z. Chen, and G.J. Qi, *Acta Mater.* 52, 2047 (2004).
22. M. He, A. Kumar, P.T. Yeo, G.J. Qi, and Z. Chen, *Thin Solid Films* 462, 387 (2004).
23. Z. Chen, M. He, and G.J. Qi, *J. Electron. Mater.* 33, 1465 (2004).
24. M.O. Alam, Y.C. Chan, and K.C. Hung, *Microelectron. Reliability* 42, 1065 (2002).
25. M.O. Alam, Y.C. Chan, and K.N. Tu, *J. Appl. Phys.* 94, 4108 (2003).
26. Y.-D. Jeon, K.-W. Paik, K.-S. Bok, W.-S. Choi, and C.-L. Cho, Studies on Ni-Sn Intermetallic Compound and P-Rich Ni Layer at the Electroless Nickel UBM-Solder Interface and Their Effects on Flip Chip Solder Joint Reliability, Electronic Component and Technology Conf., 2001 Proc., 51st, pp. 1326–1332.
27. M. He, Z. Chen, and G.J. Qi, *Metall. Mater. Trans.* A 36A, 65 (2005).
28. D.R. Frear and P.T. Vianco, *Metall. Mater. Trans.* A 25A, 1509 (1994).
29. H.T. Lee and M.H. Chen, *Mater. Sci. Eng.* A 333, 24 (2002).
30. M. McCormack, S. Jin, G.W. Kammlott, and H.S. Chen, *Appl. Phys. Lett.* 63, 15 (1993).
31. Y.C. Chan, A.C.K. So, and J.K.L. Lai, *Mater. Sci. Eng.* B55, 5 (1998).
32. R.E. Pratt, E.I. Stromswold, and D.J. Quesnel, *J. Electron. Mater.* 23, 375 (1994).
33. R.E. Pratt E.I. Stromswold D.J. Quesnel, *IEEE Trans. Components, Packaging, Manufacturing Technol.*, Part A 19, 134 (1996).